

# Production and decay of up-type and down-type new heavy quarks through anomalous interactions at the LHC

I. Turk Çakır\* and S. Kuday†

*Istanbul Aydin University, Application and Research*

*Center for Advanced Studies, 34295, Istanbul, Turkey*

O. Çakır‡

*Istanbul Aydin University, Application and Research*

*Center for Advanced Studies, 34295, Istanbul, Turkey and*

*Ankara University, Department of Physics, 06100, Ankara, Turkey*

## Abstract

We study the process  $pp \rightarrow QVX$  (where  $Q = t, b$  and  $V = g, \gamma, Z$ ) through the anomalous interactions of the new heavy quarks at the LHC. Considering the present limits on the masses and mixings, the signatures of the heavy quark anomalous interactions are discussed and analysed at the LHC for the center of mass energy of 13 TeV. An important sensitivity to anomalous couplings  $\kappa_g^{t'}/\Lambda = 0.10 \text{ TeV}^{-1}$ ,  $\kappa_\gamma^{t'}/\Lambda = 0.14 \text{ TeV}^{-1}$ ,  $\kappa_Z^{t'}/\Lambda = 0.19 \text{ TeV}^{-1}$  and  $\kappa_g^{b'}/\Lambda = 0.15 \text{ TeV}^{-1}$ ,  $\kappa_Z^{b'}/\Lambda = 0.19 \text{ TeV}^{-1}$ ,  $\kappa_\gamma^{b'}/\Lambda = 0.30 \text{ TeV}^{-1}$  for the mass of 750 GeV of the new heavy quarks  $t'$  and  $b'$  can be reached for an integrated luminosity of  $L_{int} = 100 \text{ fb}^{-1}$ .

---

\*Electronic address: [ilkayturkcakir@aydin.edu.tr](mailto:ilkayturkcakir@aydin.edu.tr)

†Electronic address: [sinankuday@aydin.edu.tr](mailto:sinankuday@aydin.edu.tr)

‡Electronic address: [ocakir@science.ankara.edu.tr](mailto:ocakir@science.ankara.edu.tr)

## I. INTRODUCTION

The standard model (SM) of the strong and electroweak interactions describes successfully the phenomena of particle physics. However, there are many unanswered questions suggesting the SM to be an effective theory. In order to answer some of the problems with the SM, additional new fermions can be accommodated in many models beyond the SM (see Refs. [1], [2], [3], [4] and references therein). The new heavy quarks could also be produced in pairs at the LHC with center of mass energy of 13 TeV. However, due to the expected smallness of the mixing between the new heavy quarks and known quarks, the decay modes can be quite different from the one relevant to charged weak interactions. A new symmetry beyond the SM is expected to explain the smallness of these mixings. The arguments given in Ref. [5] for anomalous interactions of the top quark are more valid for the new heavy quarks  $t'$  and  $b'$  due to their expected larger masses than the top quark.

The ATLAS experiment [6] and CMS experiment [7] have searched for the fourth generation of quarks and set limits on the mass of  $m_{t'} > 570$  GeV and  $m_{b'} > 470$  GeV at  $\sqrt{s} = 7$  TeV. The pair production of new heavy quarks have been searched by the ATLAS experiment [8], [9] and the  $m_{t'} > 656$  GeV mass limits are set at  $\sqrt{s} = 7$  TeV. The CMS experiment have excluded  $t'$  masses below 557 GeV[10]. The vector-like quarks have been searched by the ATLAS experiment [11], [12] and set bounds as 900 GeV for charged current channel and 760 GeV for neutral current channel at  $\sqrt{s} = 7$  TeV. The CMS experiment [13], [14] have set the lower bounds on the mass of 687 GeV at  $\sqrt{s} = 8$  TeV. Some of the final states in the searches of new phenomena [15] and excited quarks [16] can also be considered in relation with the new heavy quarks.

The anomalous resonant productions of the fourth family quarks have been studied in Refs. [17, 18] at the LHC with  $\sqrt{s} = 14$  TeV. The possible single productions of fourth generation quarks via anomalous interactions at Tevatron have also been studied in Refs. [19, 20]. The parameter space for the mixing of the fourth generation quarks have been presented in Ref. [21]. The CP violating flavour changing neutral current processes of the fourth generation quarks have been analysed in Ref. [22], and the large mixing between fourth generation and first three generations have been excluded under the proposed fit conditions. Investigation of the parameter space favoured by the precision electroweak data have been performed for the fourth SM family fermions in Ref. [23].

In this work, we present the analysis of anomalous productions and decays of new heavy quarks  $t'$  and  $b'$  at the LHC. We have performed the fast simulation for the signal and background. Any observations of the invariant mass peak in the range of  $500 - 1000$  GeV and excess in the events with the final states originating from  $tV$  and  $bV$  can be interpreted as the signal for the new heavy quarks  $t'$  and  $b'$  via the anomalous interactions.

## II. HEAVY QUARKS ANOMALOUS INTERACTIONS

A general theory that has the standard model (SM) as its low energy limit can be written as a series in  $\Lambda^{-1}$  with operators obeying the required symmetries. The effective Lagrangian for the anomalous interactions among the heavy quarks ( $Q' \equiv t'$  or  $b'$ ), ordinary quarks  $q$ , and the gauge bosons  $V = \gamma, Z, g$  can be written explicitly:

$$L = \sum_{q_i=u,c,t} \frac{\kappa_\gamma^{q_i}}{\Lambda} Q_{q_i} g_e \bar{t}' \sigma_{\mu\nu} q_i F^{\mu\nu} + \sum_{q_i=u,c,t} \frac{\kappa_z^{q_i}}{2\Lambda} g_z \bar{t}' \sigma_{\mu\nu} q_i Z^{\mu\nu} + \sum_{q_i=u,c,t} \frac{\kappa_g^{q_i}}{2\Lambda} g_s \bar{t}' \sigma_{\mu\nu} \lambda_a q_i G_a^{\mu\nu} \\ + \sum_{q_i=d,s,b} \frac{\kappa_\gamma^{q_i}}{\Lambda} Q_{q_i} g_e \bar{b}' \sigma_{\mu\nu} q_i F^{\mu\nu} + \sum_{q_i=d,s,b} \frac{\kappa_z^{q_i}}{2\Lambda} g_z \bar{b}' \sigma_{\mu\nu} q_i Z^{\mu\nu} + \sum_{q_i=d,s,b} \frac{\kappa_g^{q_i}}{2\Lambda} g_s \bar{b}' \sigma_{\mu\nu} \lambda_a q_i G_a^{\mu\nu} + h.c. \quad (1)$$

where  $F^{\mu\nu}$ ,  $Z^{\mu\nu}$  and  $G^{\mu\nu}$  are the field strength tensors of the gauge bosons;  $\sigma_{\mu\nu} = i(\gamma_\mu \gamma_\nu - \gamma_\nu \gamma_\mu)/2$ ;  $\lambda_a$  are the Gell-Mann matrices;  $Q_q$  is the electric charge of the quark ( $q$ );  $g_e$ ,  $g_z$  and  $g_s$  are the electromagnetic, neutral weak and the strong coupling constants, respectively.  $g_z = g_e / \cos \theta_w \sin \theta_w$ , where  $\theta_w$  is the weak mixing angle.  $\kappa_\gamma$  is the anomalous coupling with photon;  $\kappa_z$  is for the  $Z$  boson, and  $\kappa_g$  is the coupling with gluon. Finally,  $\Lambda$  is the cutoff scale for the new interactions.

## III. DECAY WIDTHS AND BRANCHINGS

For the decay channels  $Q' \rightarrow Vq$  where  $V \equiv \gamma, Z, g$ , we use the effective Lagrangian to calculate the anomalous decay widths

$$\Gamma(Q' \rightarrow gq) = \frac{2}{3} \left( \frac{\kappa_g^q}{\Lambda} \right)^2 \alpha_s m_{Q'}^3 \lambda_0 \quad (2)$$

$$\Gamma(Q' \rightarrow \gamma q) = \frac{1}{2} \left( \frac{\kappa_\gamma^q}{\Lambda} \right)^2 \alpha_e Q_q^2 m_{Q'}^3 \lambda_0 \quad (3)$$

$$\Gamma(Q' \rightarrow Zq) = \frac{1}{16} \left( \frac{\kappa_Z^q}{\Lambda} \right)^2 \frac{\alpha_e m_{Q'}^3}{\sin^2 \theta_W \cos^2 \theta_W} \lambda_Z \sqrt{\lambda_r} \quad (4)$$

with

$$\lambda_0 = 1 - 3m_q^2/m_{Q'}^2 + 3m_q^4/m_{Q'}^4 - m_q^6/m_{Q'}^6 \quad (5)$$

$$\lambda_r = 1 + m_W^4/m_{Q'}^4 + m_q^4/m_{Q'}^4 - 2m_W^2/m_{Q'}^2 - 2m_q^2/m_{Q'}^2 - 2m_W^2 m_q^2/m_{Q'}^4 \quad (6)$$

$$\lambda_Z = 2 - m_Z^2/m_{Q'}^2 - 4m_q^2/m_{Q'}^2 + 2m_q^4/m_{Q'}^4 - 6m_q m_Z^2/m_{Q'}^3 - m_Z^2 m_t^2/m_{Q'}^4 - m_Z^4/m_{Q'}^4 \quad (7)$$

The anomalous decay widths in different channels are proportional to  $\Lambda^{-2}$ , and they are assumed to be dominant for  $\kappa/\Lambda > 0.1 \text{ TeV}^{-1}$  over the charged current channels. In this case, if we take all the anomalous coupling equal then the branching ratios will be nearly independent of  $\kappa/\Lambda$ . We have used three parametrizations sets entitled PI, PII and PIII. For the PI parametrization, we assume the constant value  $\kappa_i/\Lambda = 0.1 \text{ TeV}^{-1}$ , and PII has the parameters  $\kappa_i/\Lambda = 0.1\lambda^{4-i} \text{ TeV}^{-1}$  with  $\lambda = 0.5$ . For PIII we take the couplings  $\kappa_i/\Lambda = 0.5\lambda^{4-i} \text{ TeV}^{-1}$  with the same value of  $\lambda$ . The index  $i$  is the generation number.

Table I and Table II present the decay width and branching ratios of the new heavy quark  $t'$  through anomalous interactions for the parametrizations PI, PII and PIII, respectively. Taking the anomalous coupling  $\kappa/\Lambda = 0.1 \text{ TeV}^{-1}$  we calculate the  $t'$  decay width  $\Gamma = 0.65 \text{ GeV}$  and  $1.90 \text{ GeV}$  for  $m_{t'} = 700 \text{ GeV}$  and  $1000 \text{ GeV}$ , respectively. The branching into  $t' \rightarrow qg$  channel is the largest and branching into  $t' \rightarrow q\gamma$  channel is the smallest for equal anomalous couplings with the parametrization PI. On the other hand, PII and PIII parametrizations give higher branching ratios into  $tV$  ( $V = g, Z, \gamma$ ) than  $qV$  ( $q = u, c$ ) channels due to  $\lambda^{4-i}$  factor in the parametrizations.

For the new heavy quark  $b'$  the decay width and branching ratios are presented in Table III and Table IV for the parametrizations PI, PII and PIII, respectively. We calculate the  $b'$  decay width, by taking the anomalous coupling  $\kappa/\Lambda = 0.1 \text{ TeV}^{-1}$ ,  $\Gamma = 0.68 \text{ GeV}$  and  $1.92 \text{ GeV}$  for  $m_{b'} = 700 \text{ GeV}$  and  $1000 \text{ GeV}$ , respectively. The branching for  $b' \rightarrow qg$  is the largest (30%) and its the smallest for  $b' \rightarrow q\gamma$  (0.2%) channel for equal anomalous couplings with the parametrization PI. For PII and PIII parametrizations the branching ratios into

Table I: Branching ratios (%) and decay width of the heavy quarks ( $t'$ ) with only anomalous interactions for PI parametrization and  $\kappa/\Lambda = 0.1$  TeV $^{-1}$ .

Mass(GeV)	$gu(c)$	$gt$	$Zu(c)$	$Zt$	$\gamma u(c)$	$\gamma t$	$\Gamma(\text{GeV})$
500	33.5	22.9	2.86	1.82	0.92	0.63	0.23
600	32.3	25.0	2.86	2.13	0.91	0.70	0.41
700	31.6	26.2	2.87	2.34	0.90	0.75	0.65
800	31.1	27.0	2.89	2.48	0.90	0.78	0.97
900	30.7	27.5	2.91	2.58	0.91	0.81	1.39
1000	30.5	27.8	2.93	2.66	0.91	0.83	1.90

Table II: The same as Table I, but for PII (PIII) parametrizations.

Mass(GeV)	$gu$	$gc$	$gt$	$Zu$	$Zc$	$Zt$	$\gamma u$	$\gamma c$	$\gamma t$	$\Gamma(\text{GeV})$
500	5.66	22.60	61.90	0.48	1.93	4.92	0.15	0.62	1.71	0.021 (0.558)
600	5.17	20.70	63.90	0.46	1.83	5.46	0.14	0.58	1.80	0.040 (1.024)
700	4.90	19.60	64.90	0.44	1.78	5.79	0.14	0.56	1.87	0.066 (1.68)
800	4.73	18.90	65.60	0.44	1.76	6.02	0.14	0.55	1.91	0.100 (2.561)
900	4.61	18.40	65.90	0.44	1.74	6.19	0.13	0.54	1.95	0.145 (3.680)
1000	4.53	18.10	66.20	0.43	1.74	6.32	0.13	0.54	1.98	0.200 (5.070)

$bV$  ( $V = g, Z, \gamma$ ) are larger than  $qV$  ( $q = d, s$ ) channels. The  $t'$  and  $b'$  decay widths are about the same values for PII and PIII parametrizations.

#### IV. THE CROSS SECTIONS

In order to study the new heavy quark productions at the LHC, we have used effective anomalous interaction vertices and implemented these vertices into the CalcHEP package [24]. In all of the numerical calculations, the parton distribution function are set to the CTEQ6L parametrization [25]. The new heavy quarks can be produced through its anomalous couplings to the ordinary quarks and neutral vector bosons as shown in Fig. 1.

Total cross sections for the productions of new heavy quarks  $t'$  and  $b'$  are given in Table V and Table VI for the parametrizations PI, PII and PIII, at the center of mass energy of 8

Table III: Branching ratios (%) and decay width of the heavy quarks ( $b'$ ) with only anomalous interactions for PI parametrization and  $\kappa/\Lambda = 0.1 \text{ TeV}^{-1}$ .

Mass(GeV)	$gd(s, b)$	$Zd(s, b)$	$\gamma d(s, b)$	$\Gamma(\text{GeV})$
500	30.50	2.60	0.21	0.257
600	30.40	2.69	0.21	0.436
700	30.40	2.76	0.22	0.682
800	30.30	2.82	0.22	1.005
900	30.20	2.86	0.22	1.415
1000	30.20	2.90	0.23	1.921

Table IV: The same as Table III, but for PII (PIII) parametrizations.

Mass(GeV)	$gd$	$gs$	$gb$	$Zd$	$Zs$	$Zb$	$\gamma d$	$\gamma s$	$\gamma b$	$\Gamma(\text{GeV})$
500	4.36	17.40	69.80	0.37	1.49	5.95	0.030	0.12	0.48	0.028 (0.704)
600	4.35	17.40	69.50	0.38	1.54	6.16	0.030	0.12	0.49	0.047 (1.194)
700	4.34	17.30	69.40	0.39	1.58	6.31	0.031	0.12	0.50	0.074 (1.866)
800	4.33	17.30	69.20	0.40	1.61	6.44	0.031	0.12	0.50	0.110 (2.749)
900	4.32	17.30	69.10	0.41	1.64	6.54	0.032	0.13	0.51	0.154 (3.869)
1000	4.32	17.30	69.00	0.41	1.66	6.63	0.032	0.13	0.52	0.210 (5.253)

TeV and 13 TeV. For an illustration, taking the mass of new heavy quarks as 700 GeV the cross section of  $t'(b')$  production is calculated as 8.50 pb (10.03 pb) for the parametrization PIII at  $\sqrt{s} = 13 \text{ TeV}$ . It can be seen from Table V and Table VI, the cross sections decreases while the mass of the new heavy quark increases. The cross section for  $t'$  production is larger than the  $b'$  production with a factor of 1.2-1.8 (0.7-1.0) for PI (PII and PIII) parametrization



Figure 1: Diagrams for the subprocess  $gq \rightarrow VQ$  with anomalous vertices  $Q'qV$  and  $Q'QV$  (where  $Q'$  can be the heavy quark  $b'$  or  $t'$  depending on the type of light ( $q$ ) or heavy ( $Q \equiv t, b$ ) quarks, respectively).

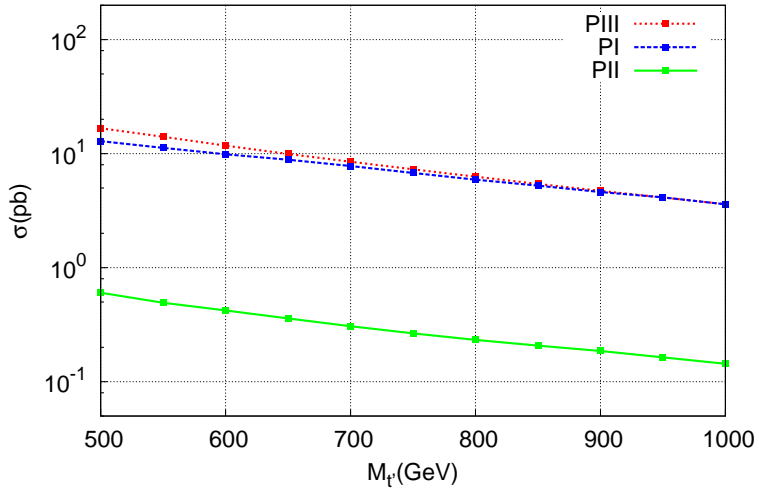


Figure 2: The cross section for the process  $pp \rightarrow tV + X$  depending on the mass for parameter sets PI, PII and PIII at the center of mass energy  $\sqrt{s} = 13$  TeV.

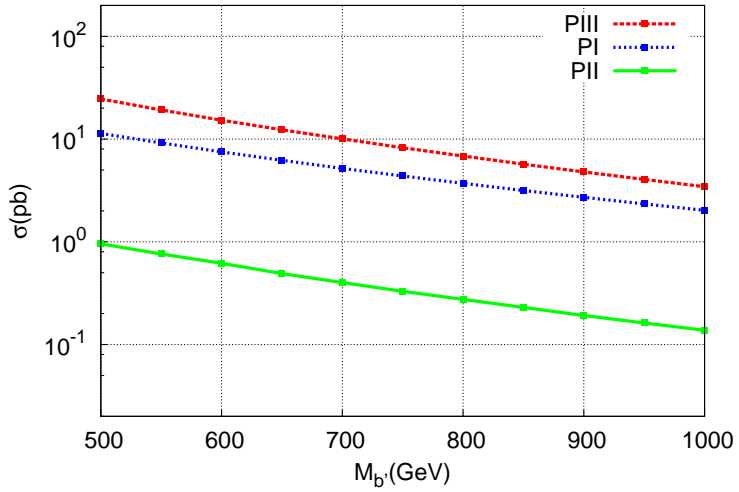


Figure 3: The cross section for the process  $pp \rightarrow bX$  depending on the new heavy quark mass for parameter sets PI, PII and PIII at the center of mass energy  $\sqrt{s} = 13$  TeV.

depending on the considered mass range at  $\sqrt{s} = 13$  TeV. The general behaviours of the production cross sections depending on the mass of heavy quarks are presented in Fig. 2 and Fig. 3 for different parametrizations.

Table V: The cross sections (in pb) of heavy quark  $t'$  production without cuts for PI, PII and PIII parametrizations at the center of mass energy 13 TeV (8 TeV), respectively.

Mass (GeV)	PI	PII	PIII
	$\sqrt{s} = 13 \text{ TeV (8 TeV)}$	$\sqrt{s} = 13 \text{ TeV (8 TeV)}$	$\sqrt{s} = 13 \text{ TeV (8 TeV)}$
500	13.733 (5.30)	0.664 (0.244)	16.736 (6.113)
600	10.362 (3.72)	0.464 (0.159)	11.770 (4.031)
700	7.825 (2.64)	0.337 (0.109)	8.502 (2.718)
800	5.961 (1.89)	0.250 (0.075)	6.276 (1.882)
900	4.602 (1.36)	0.189 (0.053)	4.701 (1.326)
1000	3.593 (0.98)	0.144 (0.038)	3.609 (0.950)

Table VI: The cross sections (in pb) of heavy quark  $b'$  production without cuts for PI, PII and PIII parametrizations at the center of mass energy of 13 TeV (8 TeV), respectively.

Mass (GeV)	PI	PII	PIII
	$\sqrt{s} = 13 \text{ TeV (8 TeV)}$	$\sqrt{s} = 13 \text{ TeV (8 TeV)}$	$\sqrt{s} = 13 \text{ TeV (8 TeV)}$
500	11.340 (3.913)	0.970 (0.285)	24.474 (7.114)
600	7.495 (2.410)	0.607 (0.162)	15.290 (4.09)
700	5.179 (1.546)	0.412 (0.099)	10.031 (2.483)
800	3.697 (1.025)	0.286 (0.062)	6.832 (1.566)
900	2.707 (0.697)	0.1905 (0.040)	4.791 (1.018)
1000	2.021 (0.482)	0.137 (0.027)	3.441 (0.678)

### A. Analysis of the process $pp \rightarrow W^+ bV + X$ ( $V = g, Z, \gamma$ ) for $t'$ signal

The signal process  $pp \rightarrow W^+ bV + X$  ( $V = g, Z, \gamma$ ) includes the  $t'$  exchange both in the  $s$ -channel and  $t$ -channel. The  $s$ -channel contribution to the signal process would appear itself as resonance around the  $t'$  mass value in the  $WbV$  invariant mass. The  $t$ -channel gives the non-resonant contribution. We consider that the  $W$  boson decays into lepton+missing transverse momentum with the branching ratio 21% and  $Z$  boson decays into dilepton with the branching 6.7%. In our analyses, we consider the  $t'$  signal in the  $l + b_{jet} + \gamma + MET$ ,  $l + b_{jet} + j + MET$  and  $3l + b_{jet} + MET$  channels, where  $l = e, \mu$ . However, if one takes the

hadronic  $W$  decays the signal will be enhanced by a factor of  $BR(W \rightarrow \text{hadrons})/BR(W \rightarrow l\nu)$ .

We have obtained the cross sections by using the cuts pseudorapidity  $|\eta_{j,\gamma}| < 2.5$  and transverse momentum  $p_T^{j,\gamma} > 20 - 200$  GeV for jets and photon, in Table VII (Table VIII, Table IX) for PI (PII, PIII) parametrizations, respectively. It appears from signal significance calculations that the optimized transverse momentum cut is  $p_T > 100$  GeV for  $t'$  analyses.

The backgrounds for the final state  $W^+ b(\bar{b}) V$  (where  $V \equiv$  photon, jet and  $Z$  boson) are given in Table X. We apply the following cuts to the final state photon and jets as  $|\eta_{j,\gamma}| < 2.5$  and  $p_T^{j,\gamma} > 20 - 200$  GeV. For the background cross section estimates, we assume the efficiency for  $b$ -tagging to be  $\varepsilon_b = 50\%$ , and the rejection ratios 10% for  $c$  ( $\bar{c}$ ) quark jets and 1% for light quark jets since they are assumed to be mistagged as  $b$ -jets.

In order to find the discovery limits we use the statistical significance as

$$SS = \sqrt{2 \left[ (S + B) \ln(1 + \frac{S}{B}) - S \right]} \quad (8)$$

where  $S$  and  $B$  are the numbers of the signal and background events, respectively. In Figs. 4- 6, the integrated luminosity required to reach  $3\sigma$  significance for the signal of  $t'$  anomalous interactions is shown for parametrization PI, PII and PIII at the LHC with  $\sqrt{s} = 13$  TeV. It is seen from these figures that the channel  $t' \rightarrow tZ$  requires more integrated luminosity than the other channels. By requiring the signal significance  $SS = 3$ , the contour plots of  $\kappa/\Lambda$  and mass of  $t'$  quark are presented in Fig. 7. The results show that one can discover the  $t'$  quark anomalous couplings  $\kappa/\Lambda$  down to  $0.1 \text{ TeV}^{-1}$  in the  $tg$  channel for  $m_{t'} = 750$  GeV.

## B. Analysis of the process $pp \rightarrow bV + X$ ( $V = g, Z, \gamma$ ) for $b'$ signal

The signal process  $pp \rightarrow bV + X$  ( $V = g, Z, \gamma$ ) includes the new heavy quark  $b'$  exchange both in the  $s$ -channel and  $t$ -channel. The  $s$ - channel contributes to the signal process as resonance around the  $b'$  mass value in the  $bV$  invariant mass, while the  $t$ - channel contributes to the non-resonant behaviour. For this process, we consider the leptonic decays of  $Z$  boson. In the analyses, we consider the  $b'$  signal to be  $b_{jet} + \gamma$ ,  $b_{jet} + j$  and  $b_{jet} + \text{dilepton}$ .

We have obtained the cross sections by using the pseudorapidity cuts  $|\eta_{j,\gamma}| < 2.5$  and transverse momentum cuts  $p_T^{j,\gamma} > 20 - 200$  GeV for jets and photon, in Table XI (Table XII, Table XIII) for PI (PII, PIII) parametrizations, respectively. It appears from signal

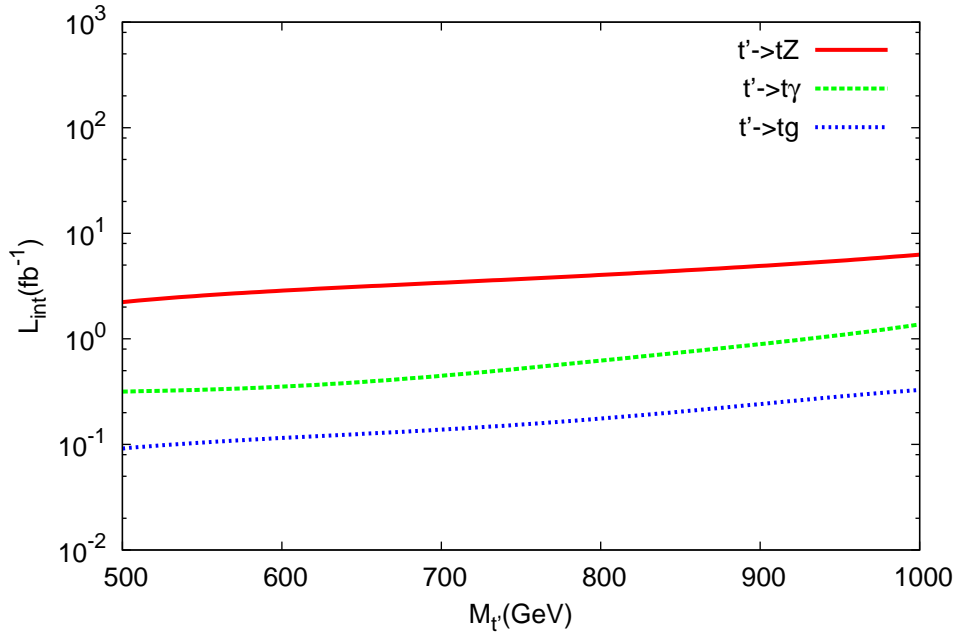


Figure 4: Integrated luminosity required to reach  $3\sigma$  significance for the signal of  $t'$  anomalous interactions for parametrization PI at the LHC with  $\sqrt{s} = 13$  TeV.

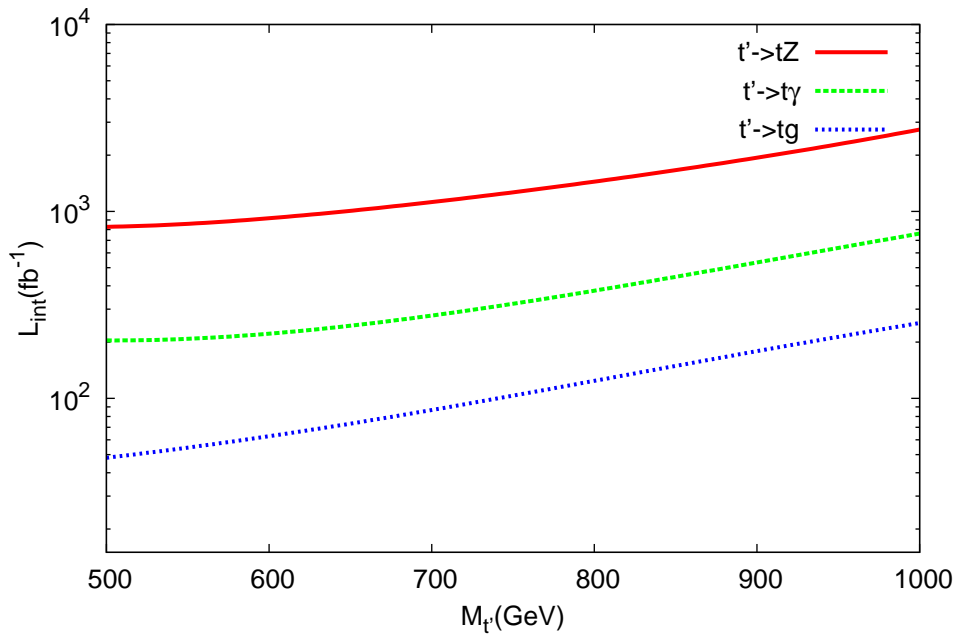


Figure 5: The same as Fig.4, but for parametrization PII.

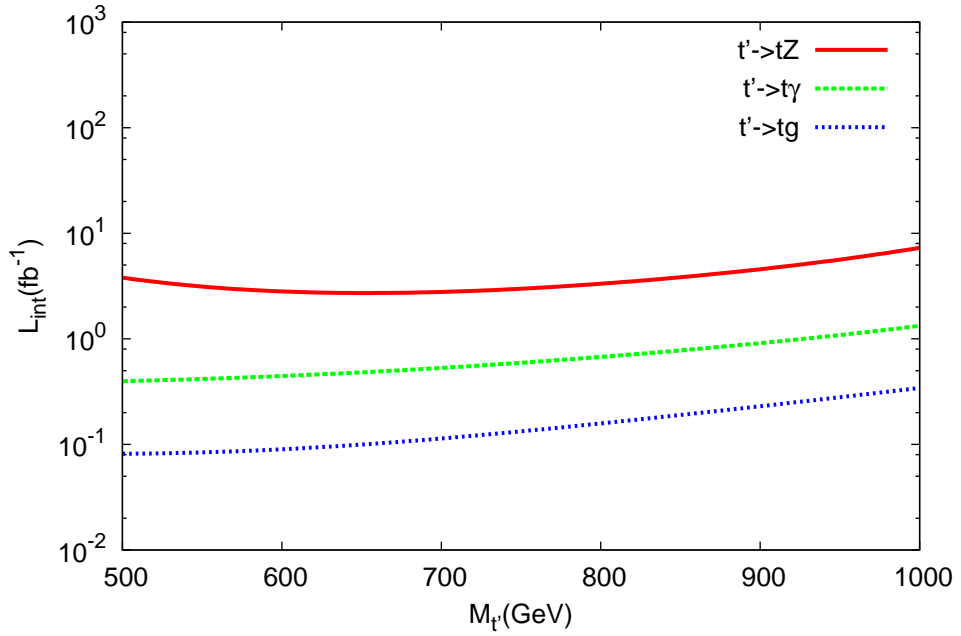


Figure 6: The same as Fig. 4, but for parametrization PIII.

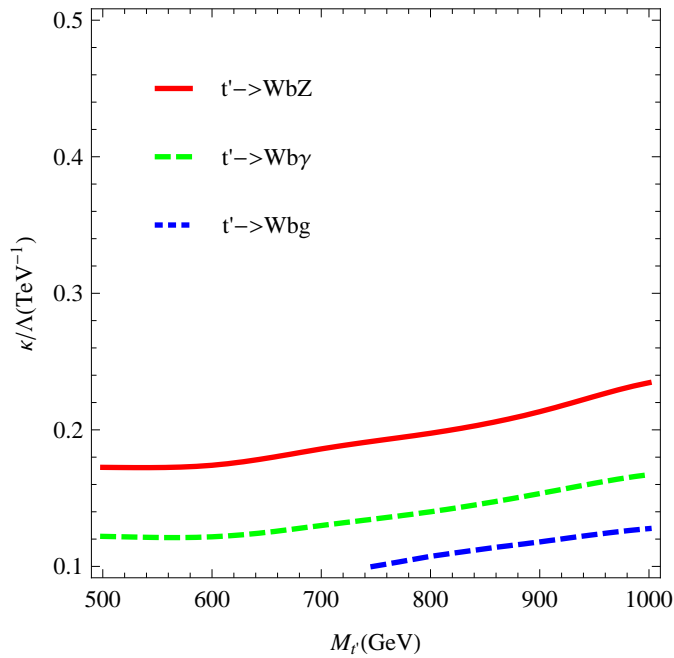


Figure 7: The contour plot of anomalous coupling and mass of new heavy quark  $t'$  for the dynamical parametrization explained in the text with a significance  $3\sigma$  at  $\sqrt{s} = 13$  TeV and  $L_{int} = 100$  fb $^{-1}$ .

Table VII: The cross sections (in pb) for  $t'$  signal in different decay channels for PI parametrization with  $p_T$  cuts on the jets and photon and  $|\eta_{j,\gamma}| < 2.5$  at the center of mass energy  $\sqrt{s} = 13$  TeV.

Signal	PI			
	$p_T > 20$ GeV	$p_T > 50$ GeV	$p_T > 100$ GeV	$p_T > 200$ GeV
$pp \rightarrow W^+ b\gamma X$				
500	$2.89 \times 10^{-1}$	$2.10 \times 10^{-1}$	$1.24 \times 10^{-1}$	$1.02 \times 10^{-4}$
600	$2.43 \times 10^{-1}$	$1.64 \times 10^{-1}$	$1.19 \times 10^{-1}$	$1.23 \times 10^{-2}$
700	$1.68 \times 10^{-1}$	$1.2 \times 10^{-1}$	$1.12 \times 10^{-1}$	$2.25 \times 10^{-2}$
800	$1.30 \times 10^{-1}$	$1.03 \times 10^{-1}$	$7.53 \times 10^{-2}$	$3.25 \times 10^{-2}$
900	$1.02 \times 10^{-1}$	$8.08 \times 10^{-2}$	$6.96 \times 10^{-2}$	$3.02 \times 10^{-2}$
1000	$7.61 \times 10^{-2}$	$6.35 \times 10^{-2}$	$5.07 \times 10^{-2}$	$2.94 \times 10^{-2}$
$pp \rightarrow W^+ bgX$				
500	$7.78 \times 10^0$	$6.02 \times 10^0$	$3.63 \times 10^0$	$4.74 \times 10^{-3}$
600	$6.30 \times 10^0$	$5.18 \times 10^0$	$3.13 \times 10^0$	$2.58 \times 10^{-1}$
700	$4.99 \times 10^0$	$3.63 \times 10^0$	$3.04 \times 10^0$	$9.32 \times 10^{-1}$
800	$4.01 \times 10^0$	$3.45 \times 10^0$	$2.76 \times 10^0$	$9.91 \times 10^{-1}$
900	$3.32 \times 10^0$	$2.77 \times 10^0$	$2.13 \times 10^0$	$1.08 \times 10^0$
1000	$2.58 \times 10^0$	$2.27 \times 10^0$	$1.88 \times 10^0$	$1.01 \times 10^0$
$pp \rightarrow W^+ bZX$				
500	$7.96 \times 10^{-1}$	$6.01 \times 10^{-1}$	$3.01 \times 10^{-1}$	$1.01 \times 10^{-4}$
600	$4.79 \times 10^{-1}$	$3.86 \times 10^{-1}$	$2.45 \times 10^{-1}$	$2.71 \times 10^{-3}$
700	$3.99 \times 10^{-1}$	$3.12 \times 10^{-1}$	$2.39 \times 10^{-1}$	$6.96 \times 10^{-2}$
800	$3.31 \times 10^{-1}$	$2.89 \times 10^{-1}$	$2.09 \times 10^{-1}$	$8.05 \times 10^{-2}$
900	$2.73 \times 10^{-1}$	$2.73 \times 10^{-1}$	$1.91 \times 10^{-1}$	$9.54 \times 10^{-2}$
1000	$2.23 \times 10^{-1}$	$2.02 \times 10^{-1}$	$1.61 \times 10^{-1}$	$9.10 \times 10^{-2}$

significance calculation that the optimized transverse momentum cut is  $p_T > 200$  GeV for  $b'$  analyses.

The backgrounds for the final state  $b(\bar{b})V$  (where  $V$  =photon, jet and  $Z$  boson) are given in XIV. We apply the following cuts to the final state photon and jets as  $|\eta_{j,\gamma}| < 2.5$  and  $p_T^{j,\gamma} > 20 - 200$  GeV. It can be noted that the background cross section decreases as the  $p_T$

Table VIII: The same as Table VII, but for parametrization PII.

Signal	PII			
	$p_T > 20 \text{ GeV}$	$p_T > 50 \text{ GeV}$	$p_T > 100 \text{ GeV}$	$p_T > 200 \text{ GeV}$
$pp \rightarrow W^+ b\gamma X$				
500	$6.78 \times 10^{-3}$	$5.07 \times 10^{-3}$	$3.45 \times 10^{-3}$	$2.64 \times 10^{-7}$
600	$6.57 \times 10^{-3}$	$5.42 \times 10^{-3}$	$3.47 \times 10^{-3}$	$5.34 \times 10^{-4}$
700	$5.02 \times 10^{-3}$	$4.31 \times 10^{-3}$	$3.04 \times 10^{-3}$	$8.73 \times 10^{-4}$
800	$3.91 \times 10^{-3}$	$3.76 \times 10^{-3}$	$2.56 \times 10^{-3}$	$1.03 \times 10^{-3}$
900	$3.03 \times 10^{-3}$	$2.68 \times 10^{-3}$	$2.11 \times 10^{-3}$	$1.01 \times 10^{-3}$
1000	$2.40 \times 10^{-3}$	$2.43 \times 10^{-3}$	$1.77 \times 10^{-3}$	$9.98 \times 10^{-4}$
$pp \rightarrow W^+ bgX$				
500	$3.47 \times 10^{-1}$	$2.68 \times 10^{-1}$	$1.52 \times 10^{-1}$	$5.30 \times 10^{-6}$
600	$2.51 \times 10^{-1}$	$2.12 \times 10^{-1}$	$1.35 \times 10^{-1}$	$2.01 \times 10^{-2}$
700	$1.87 \times 10^{-1}$	$1.6 \times 10^{-1}$	$1.16 \times 10^{-1}$	$3.42 \times 10^{-2}$
800	$1.46 \times 10^{-1}$	$1.25 \times 10^{-1}$	$9.39 \times 10^{-2}$	$4.03 \times 10^{-2}$
900	$1.12 \times 10^{-1}$	$1.08 \times 10^{-1}$	$7.80 \times 10^{-2}$	$3.86 \times 10^{-2}$
1000	$9.35 \times 10^{-2}$	$8.37 \times 10^{-2}$	$6.62 \times 10^{-2}$	$3.68 \times 10^{-2}$
$pp \rightarrow W^+ bZX$				
500	$2.10 \times 10^{-2}$	$1.77 \times 10^{-2}$	$1.16 \times 10^{-2}$	$2.64 \times 10^{-7}$
600	$1.95 \times 10^{-2}$	$1.75 \times 10^{-2}$	$1.14 \times 10^{-2}$	$1.34 \times 10^{-3}$
700	$1.73 \times 10^{-2}$	$1.43 \times 10^{-2}$	$1.00 \times 10^{-2}$	$2.9 \times 10^{-3}$
800	$1.34 \times 10^{-2}$	$1.19 \times 10^{-2}$	$8.89 \times 10^{-3}$	$3.42 \times 10^{-3}$
900	$1.06 \times 10^{-2}$	$9.55 \times 10^{-3}$	$7.63 \times 10^{-3}$	$3.37 \times 10^{-3}$
1000	$8.09 \times 10^{-3}$	$7.58 \times 10^{-3}$	$6.31 \times 10^{-3}$	$3.23 \times 10^{-3}$

cuts increases. We assume the efficiency for  $b$ -tagging to be  $\varepsilon_b = 50\%$ , and the rejection ratios 10% for  $c$  ( $\bar{c}$ ) quark jets and 1% for light quark jets.

In order to reach  $3\sigma$  significance for the signal of  $b'$  anomalous interactions the required integrated luminosity is shown in Figs. 8- 10 for parametrizations PI, PII and PIII at the LHC with  $\sqrt{s} = 13 \text{ TeV}$ . The channel  $b' \rightarrow b\gamma$  requires more integrated luminosity than the other channels. By requiring the signal significance  $SS = 3$ , the contour plots of  $\kappa/\Lambda$  and

Table IX: The same as Table VII, but for parametrization PIII.

Signal	PIII			
	$p_T > 20 \text{ GeV}$	$p_T > 50 \text{ GeV}$	$p_T > 100 \text{ GeV}$	$p_T > 200 \text{ GeV}$
$pp \rightarrow W^+ b\gamma X$				
500	$2.60 \times 10^{-1}$	$2.78 \times 10^{-1}$	$1.08 \times 10^{-1}$	$1.59 \times 10^{-4}$
600	$1.78 \times 10^{-1}$	$1.61 \times 10^{-1}$	$1.01 \times 10^{-1}$	$1.42 \times 10^{-2}$
700	$1.56 \times 10^{-1}$	$1.35 \times 10^{-1}$	$9.33 \times 10^{-2}$	$2.72 \times 10^{-2}$
800	$1.17 \times 10^{-1}$	$1.06 \times 10^{-1}$	$7.84 \times 10^{-2}$	$3.32 \times 10^{-2}$
900	$9.04 \times 10^{-2}$	$8.42 \times 10^{-2}$	$6.68 \times 10^{-2}$	$3.25 \times 10^{-2}$
1000	$7.6 \times 10^{-2}$	$6.76 \times 10^{-2}$	$5.16 \times 10^{-2}$	$3.17 \times 10^{-2}$
$pp \rightarrow W^+ bgX$				
500	$8.39 \times 10^0$	$6.49 \times 10^0$	$3.86 \times 10^0$	$4.65 \times 10^{-3}$
600	$6.10 \times 10^0$	$5.78 \times 10^0$	$3.81 \times 10^0$	$5.56 \times 10^{-1}$
700	$5.39 \times 10^0$	$4.64 \times 10^0$	$3.41 \times 10^0$	$9.70 \times 10^{-1}$
800	$3.94 \times 10^0$	$3.54 \times 10^0$	$2.73 \times 10^0$	$1.05 \times 10^0$
900	$3.24 \times 10^0$	$2.76 \times 10^0$	$2.27 \times 10^0$	$1.07 \times 10^0$
1000	$2.33 \times 10^0$	$2.29 \times 10^0$	$1.84 \times 10^0$	$9.98 \times 10^{-1}$
$pp \rightarrow W^+ bZX$				
500	$7.72 \times 10^{-1}$	$1.01 \times 10^0$	$2.17 \times 10^{-1}$	$6.27 \times 10^{-4}$
600	$6.24 \times 10^{-1}$	$3.85 \times 10^{-1}$	$2.92 \times 10^{-1}$	$3.20 \times 10^{-2}$
700	$5.00 \times 10^{-1}$	$3.05 \times 10^{-1}$	$2.86 \times 10^{-1}$	$5.80 \times 10^{-2}$
800	$3.78 \times 10^{-1}$	$2.50 \times 10^{-1}$	$2.42 \times 10^{-1}$	$9.64 \times 10^{-2}$
900	$3.04 \times 10^{-1}$	$1.67 \times 10^{-1}$	$2.06 \times 10^{-1}$	$9.62 \times 10^{-2}$
1000	$2.51 \times 10^{-1}$	$1.29 \times 10^{-1}$	$1.48 \times 10^{-1}$	$9.61 \times 10^{-2}$

mass of  $b'$  quark are presented in Fig. 11. The results show that one can discover the  $b'$  quark anomalous couplings down to 0.1 in the  $bg$  channel for  $m_{b'}=500 \text{ GeV}$ .

## V. CONCLUSION

The new heavy quarks of up-type and down-type can be produced with large numbers at the LHC if they have the anomalous couplings (via flavour changing neutral current)

Table X: The cross sections (in pb) for the relevant backgrounds ( $W^+b(\bar{b})V$ ,  $W^+c(\bar{c})V$  and  $W^+jV$ , where  $V$  =photon, jet and  $Z$  boson) with  $p_T$  cuts on the jets at the center of mass energy  $\sqrt{s} = 13$  TeV.

Background	$p_T > 20$ GeV	$p_T > 50$ GeV	$p_T > 100$ GeV	$p_T > 200$ GeV
$pp \rightarrow W^+b\gamma$	$2.37 \times 10^{-3}$	$3.62 \times 10^{-4}$	$6.17 \times 10^{-5}$	$6.99 \times 10^{-6}$
$pp \rightarrow W^+\bar{c}\gamma$	$4.15 \times 10^0$	$4.59 \times 10^{-1}$	$6.25 \times 10^{-2}$	$6.21 \times 10^{-3}$
$pp \rightarrow W^+j\gamma$	$2.63 \times 10^1$	$4.30 \times 10^0$	$7.33 \times 10^{-1}$	$1.27 \times 10^{-1}$
$pp \rightarrow W^+b(\bar{b})j$	$7.26 \times 10^1$	$3.02 \times 10^1$	$6.11 \times 10^0$	$9.74 \times 10^{-1}$
$pp \rightarrow W^+c(\bar{c})j$	$5.98 \times 10^2$	$9.65 \times 10^1$	$1.79 \times 10^1$	$2.42 \times 10^0$
$pp \rightarrow W^+jj$	$7.31 \times 10^3$	$7.78 \times 10^2$	$1.61 \times 10^2$	$2.58 \times 10^1$
$pp \rightarrow W^+bZ$	$6.26 \times 10^{-4}$	$3.99 \times 10^{-4}$	$1.93 \times 10^{-4}$	$4.71 \times 10^{-5}$
$pp \rightarrow W^+\bar{c}Z$	$5.29 \times 10^{-1}$	$3.40 \times 10^{-1}$	$1.66 \times 10^{-1}$	$4.15 \times 10^{-2}$
$pp \rightarrow W^+jZ$	$8.59 \times 10^0$	$4.83 \times 10^0$	$2.49 \times 10^0$	$7.91 \times 10^{-1}$

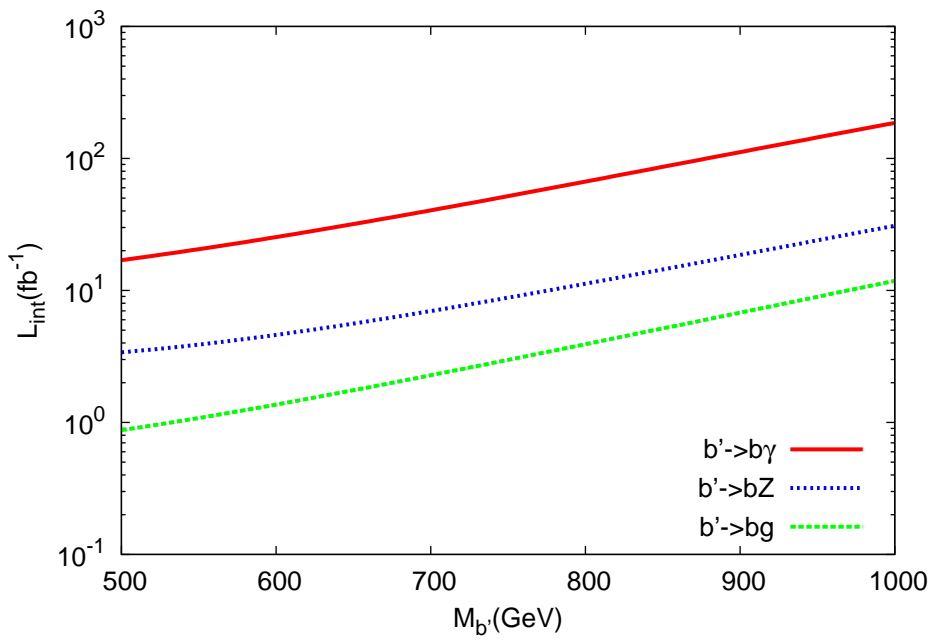


Figure 8: Integrated luminosity required to reach  $3\sigma$  significance for the signal of  $b'$  anomalous interactions for parametrization PI at the LHC with  $\sqrt{s} = 13$  TeV.

Table XI: The cross sections (in pb) for  $b'$  signal in different decay channel for parametrization PI with  $p_T$  cuts on the jets and photon and  $|\eta_{j,\gamma}| < 2.5$  at the center of mass energy  $\sqrt{s} = 13$  TeV.

Signal	PI				
	$pp \rightarrow b\gamma X$	$p_T > 20$ GeV	$p_T > 50$ GeV	$p_T > 100$ GeV	$p_T > 200$ GeV
500	$5.64 \times 10^{-2}$	$5.62 \times 10^{-2}$	$5.49 \times 10^{-2}$	$3.95 \times 10^{-2}$	
600	$3.96 \times 10^{-2}$	$3.96 \times 10^{-2}$	$3.90 \times 10^{-2}$	$3.33 \times 10^{-2}$	
700	$2.87 \times 10^{-2}$	$2.87 \times 10^{-2}$	$2.86 \times 10^{-2}$	$2.59 \times 10^{-2}$	
800	$2.12 \times 10^{-2}$	$2.13 \times 10^{-2}$	$2.12 \times 10^{-2}$	$1.99 \times 10^{-2}$	
900	$1.60 \times 10^{-2}$	$1.60 \times 10^{-2}$	$1.60 \times 10^{-2}$	$1.53 \times 10^{-2}$	
1000	$1.22 \times 10^{-2}$	$1.22 \times 10^{-2}$	$1.22 \times 10^{-2}$	$1.19 \times 10^{-2}$	
$pp \rightarrow bgX$					
500	$8.13 \times 10^0$	$8.13 \times 10^0$	$7.93 \times 10^0$	$5.96 \times 10^0$	
600	$5.59 \times 10^0$	$5.59 \times 10^0$	$5.53 \times 10^0$	$4.88 \times 10^0$	
700	$3.98 \times 10^0$	$3.98 \times 10^0$	$3.96 \times 10^0$	$3.73 \times 10^0$	
800	$2.91 \times 10^0$	$2.91 \times 10^0$	$2.90 \times 10^0$	$2.81 \times 10^0$	
900	$2.16 \times 10^0$	$2.16 \times 10^0$	$2.16 \times 10^0$	$2.14 \times 10^0$	
1000	$1.64 \times 10^0$	$1.63 \times 10^0$	$1.63 \times 10^0$	$1.62 \times 10^0$	
$pp \rightarrow bZX$					
500	$7.87 \times 10^{-1}$	$7.81 \times 10^{-1}$	$7.50 \times 10^{-1}$	$4.79 \times 10^{-1}$	
600	$5.48 \times 10^{-1}$	$5.48 \times 10^{-1}$	$5.31 \times 10^{-1}$	$4.27 \times 10^{-1}$	
700	$3.95 \times 10^{-1}$	$3.94 \times 10^{-1}$	$3.86 \times 10^{-1}$	$3.39 \times 10^{-1}$	
800	$2.92 \times 10^{-1}$	$2.91 \times 10^{-1}$	$2.86 \times 10^{-1}$	$2.61 \times 10^{-1}$	
900	$2.18 \times 10^{-1}$	$2.18 \times 10^{-1}$	$2.15 \times 10^{-1}$	$2.02 \times 10^{-1}$	
1000	$1.66 \times 10^{-1}$	$1.66 \times 10^{-1}$	$1.64 \times 10^{-1}$	$1.56 \times 10^{-1}$	

that well dominate over the charged current interactions. The single production of new heavy quarks can be achieved through the anomalous interactions at the LHC with  $\sqrt{s} = 13$  TeV. The anomalous vertices could appear significantly at leading order processes due to the possibility of new heavy quarks. From the results of signal significance calculations for  $t'$  ( $b'$ ) anomalous productions, the sensitivity to the anomalous couplings  $\kappa^{t'}/\Lambda$  ( $\kappa^{b'}/\Lambda$ ) can be

Table XII: The same as Table XI, but for parametrization PII.

Signal	PII			
	$p_T > 20 \text{ GeV}$	$p_T > 50 \text{ GeV}$	$p_T > 100 \text{ GeV}$	$p_T > 200 \text{ GeV}$
$pp \rightarrow b\gamma X$				
500	$5.18 \times 10^{-3}$	$5.26 \times 10^{-3}$	$5.04 \times 10^{-3}$	$3.54 \times 10^{-3}$
600	$3.38 \times 10^{-3}$	$3.37 \times 10^{-3}$	$3.36 \times 10^{-3}$	$2.77 \times 10^{-3}$
700	$2.32 \times 10^{-3}$	$2.31 \times 10^{-3}$	$2.30 \times 10^{-3}$	$2.05 \times 10^{-3}$
800	$1.71 \times 10^{-3}$	$1.63 \times 10^{-3}$	$1.64 \times 10^{-3}$	$1.50 \times 10^{-3}$
900	$1.17 \times 10^{-3}$	$1.16 \times 10^{-3}$	$1.17 \times 10^{-3}$	$1.11 \times 10^{-3}$
1000	$8.60 \times 10^{-4}$	$8.58 \times 10^{-4}$	$8.55 \times 10^{-4}$	$8.24 \times 10^{-4}$
$pp \rightarrow bgX$				
500	$7.40 \times 10^{-1}$	$7.39 \times 10^{-1}$	$7.21 \times 10^{-1}$	$5.16 \times 10^{-1}$
600	$4.83 \times 10^{-1}$	$4.80 \times 10^{-1}$	$4.81 \times 10^{-1}$	$3.98 \times 10^{-1}$
700	$3.22 \times 10^{-1}$	$3.22 \times 10^{-1}$	$3.20 \times 10^{-1}!$	$2.89 \times 10^{-1}!$
800	$2.24 \times 10^{-1}$	$2.21 \times 10^{-1}$	$2.21 \times 10^{-1}$	$2.04 \times 10^{-1}$
900	$1.5 \times 10^{-1}$	$1.58 \times 10^{-1}$	$1.58 \times 10^{-1}$	$1.49 \times 10^{-1}$
1000	$1.14 \times 10^{-1}$	$1.14 \times 10^{-1}$	$1.13 \times 10^{-1}$	$1.10 \times 10^{-1}$
$pp \rightarrow bZX$				
500	$6.89 \times 10^{-2}$	$6.85 \times 10^{-2}$	$6.45 \times 10^{-2}$	$4.23 \times 10^{-2}$
600	$4.52 \times 10^{-2}$	$4.51 \times 10^{-2}$	$4.34 \times 10^{-2}$	$3.53 \times 10^{-2}$
700	$3.12 \times 10^{-2}$	$3.11 \times 10^{-2}$	$3.05 \times 10^{-2}$	$2.65 \times 10^{-2}$
800	$2.19 \times 10^{-2}$	$2.18 \times 10^{-2}$	$2.15 \times 10^{-2}$	$1.95 \times 10^{-2}$
900	$1.56 \times 10^{-2}$	$1.56 \times 10^{-2}$	$1.55 \times 10^{-2}$	$1.44 \times 10^{-2}$
1000	$1.14 \times 10^{-2}$	$1.13 \times 10^{-2}$	$1.13 \times 10^{-2}$	$1.07 \times 10^{-2}$

reached down to  $0.1 \text{ TeV}^{-1}$  ( $0.15 \text{ TeV}^{-1}$ ) in the lepton+ $b$ -jet+jet+ $MET$  ( $b$ -jet+jet) channel at  $\sqrt{s} = 13 \text{ TeV}$ , assuming a dynamical parametrization for the anomalous couplings and the mass of 750 GeV for the new heavy quarks.

Table XIII: The same as Table XI, but for parametrization PIII.

Signal	PIII			
	$p_T > 20 \text{ GeV}$	$p_T > 50 \text{ GeV}$	$p_T > 100 \text{ GeV}$	$p_T > 200 \text{ GeV}$
$pp \rightarrow b\gamma X$				
500	$13.1 \times 10^{-2}$	$13.14 \times 10^{-2}$	$12.75 \times 10^{-2}$	$8.92 \times 10^{-2}$
600	$8.59 \times 10^{-2}$	$8.58 \times 10^{-2}$	$8.44 \times 10^{-2}$	$7.03 \times 10^{-2}$
700	$5.82 \times 10^{-2}$	$5.82 \times 10^{-2}$	$5.77 \times 10^{-2}$	$5.17 \times 10^{-2}$
800	$4.07 \times 10^{-2}$	$4.07 \times 10^{-2}$	$4.06 \times 10^{-2}$	$3.77 \times 10^{-2}$
900	$2.92 \times 10^{-2}$	$2.92 \times 10^{-2}$	$2.91 \times 10^{-2}$	$2.77 \times 10^{-2}$
1000	$2.14 \times 10^{-2}$	$2.13 \times 10^{-2}$	$2.13 \times 10^{-2}$	$2.06 \times 10^{-2}$
$pp \rightarrow bgX$				
500	$19.04 \times 10^0$	$18.96 \times 10^0$	$18.43 \times 10^0$	$12.86 \times 10^0$
600	$12.19 \times 10^0$	$12.13 \times 10^0$	$11.93 \times 10^0$	$9.92 \times 10^0$
700	$8.08 \times 10^0$	$8.07 \times 10^0$	$8.02 \times 10^0$	$7.17 \times 10^0$
800	$5.57 \times 10^0$	$5.57 \times 10^0$	$5.55 \times 10^0$	$5.15 \times 10^0$
900	$3.94 \times 10^0$	$3.94 \times 10^0$	$3.94 \times 10^0$	$3.74 \times 10^0$
1000	$2.85 \times 10^0$	$2.85 \times 10^0$	$2.85 \times 10^0$	$2.74 \times 10^0$
$pp \rightarrow bZX$				
500	$1.76 \times 10^0$	$1.75 \times 10^0$	$1.65 \times 10^0$	$1.05 \times 10^0$
600	$1.15 \times 10^0$	$1.14 \times 10^0$	$1.11 \times 10^0$	$8.80 \times 10^{-1}$
700	$7.83 \times 10^{-1}$	$7.80 \times 10^{-1}$	$7.60 \times 10^{-1}$	$6.61 \times 10^{-1}$
800	$5.47 \times 10^{-1}$	$5.41 \times 10^{-1}$	$5.31 \times 10^{-1}$	$4.80 \times 10^{-1}$
900	$3.92 \times 10^{-1}$	$3.90 \times 10^{-1}$	$3.82 \times 10^{-1}$	$3.60 \times 10^{-1}$
1000	$2.86 \times 10^{-1}$	$2.82 \times 10^{-1}$	$2.80 \times 10^{-1}$	$2.62 \times 10^{-1}$

Table XIV: The cross sections (in pb) for the backgrounds ( $b(\bar{b})V$ ,  $c(\bar{c})V$  and  $jV$ , where  $V$  =photon, jet and  $Z$  boson) with  $p_T$  cuts on the jets and photon at the center of mass energy  $\sqrt{s} = 13$  TeV.

Background	$p_T > 20$ GeV	$p_T > 50$ GeV	$p_T > 100$ GeV	$p_T > 200$ GeV
$pp \rightarrow b(\bar{b})\gamma X$	$2.99 \times 10^3$	$1.35 \times 10^2$	$9.04 \times 10^0$	$4.02 \times 10^{-1}$
$pp \rightarrow c(\bar{c})\gamma X$	$1.87 \times 10^4$	$8.15 \times 10^2$	$5.40 \times 10^1$	$2.43 \times 10^0$
$pp \rightarrow j\gamma X$	$5.43 \times 10^4$	$3.27 \times 10^3$	$3.38 \times 10^2$	$2.85 \times 10^1$
$pp \rightarrow b(\bar{b})jX$	$7.83 \times 10^6$	$3.05 \times 10^5$	$1.92 \times 10^4$	$8.93 \times 10^2$
$pp \rightarrow c(\bar{c})jX$	$1.22 \times 10^7$	$4.55 \times 10^5$	$2.89 \times 10^4$	$1.35 \times 10^3$
$pp \rightarrow jjX$	$2.43 \times 10^8$	$8.54 \times 10^6$	$5.44 \times 10^5$	$2.80 \times 10^4$
$pp \rightarrow b(\bar{b})ZX$	$5.02 \times 10^2$	$1.35 \times 10^2$	$2.25 \times 10^1$	$1.56 \times 10^0$
$pp \rightarrow c(\bar{c})ZX$	$5.96 \times 10^2$	$1.58 \times 10^2$	$2.64 \times 10^1$	$1.83 \times 10^0$
$pp \rightarrow jZX$	$8.00 \times 10^3$	$2.08 \times 10^3$	$4.08 \times 10^2$	$4.12 \times 10^1$

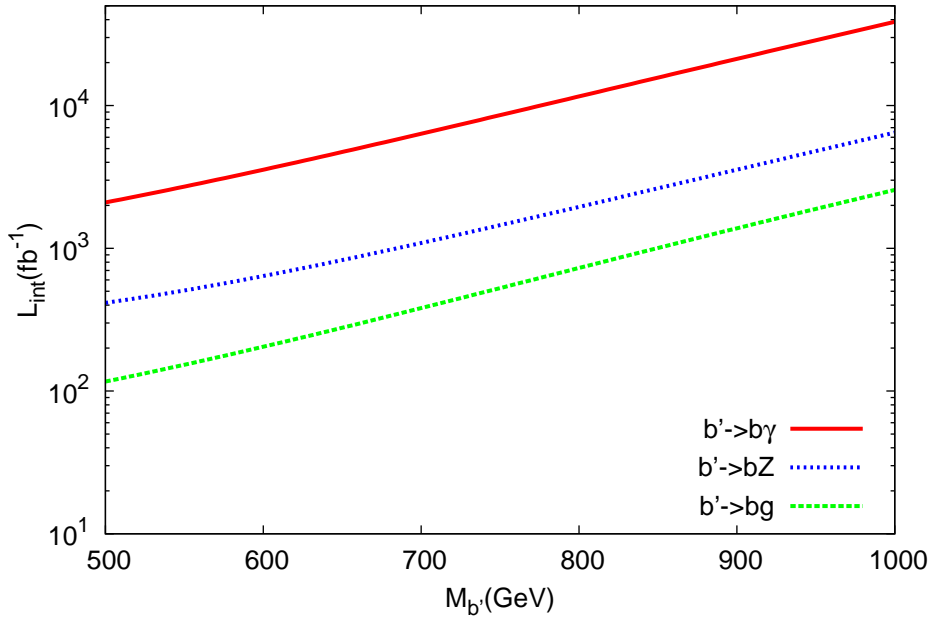


Figure 9: The same as Fig. 8, but for parametrization PII.

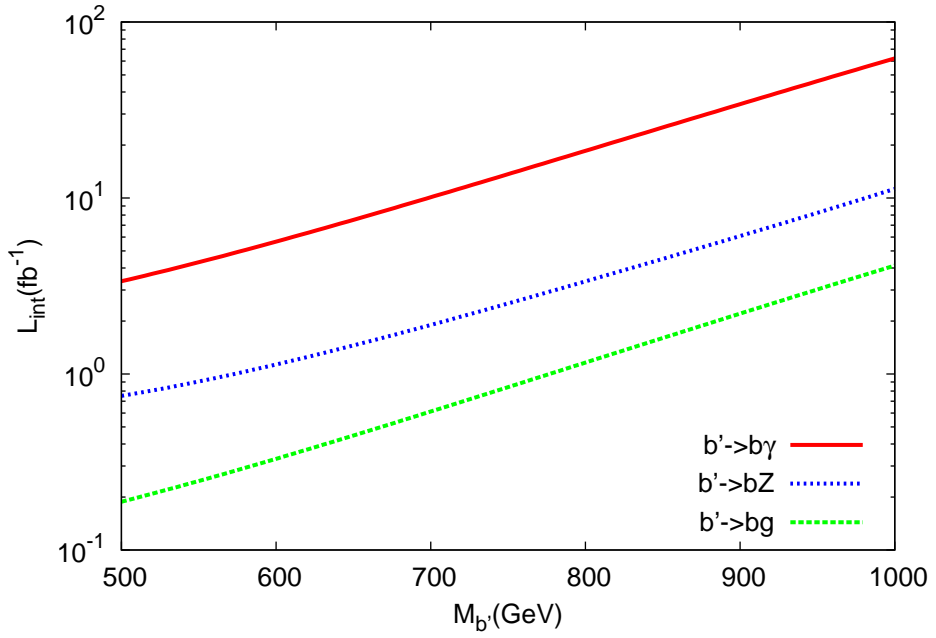


Figure 10: The same as Fig. 8, but for parametrization PIII.

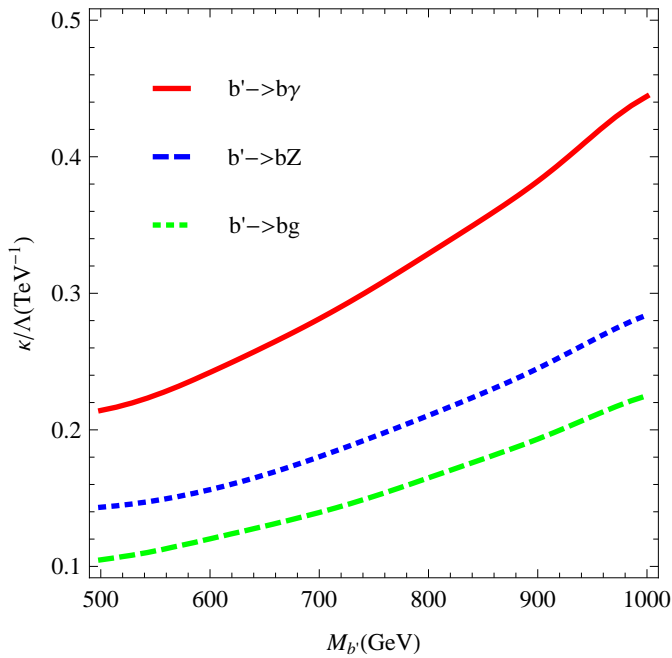


Figure 11: The contour plot of anomalous coupling and mass of new heavy quark  $b'$  for the dynamical parametrization explained in the text with a significance  $3\sigma$  at  $\sqrt{s} = 13$  TeV and  $L_{\text{int}} = 100 \text{ fb}^{-1}$ .

## Acknowledgments

This work was supported in part by Turkish Atomic Energy Authority (TAEA) under the project Grant No. 2011TAEKCERN-A5.H2.P1.01-19.

---

- [1] B. Holdom *et al.* PMC Phys. A **3**, 4 (2009).
- [2] A. Atre *et al.* Phys. Rev. D **79**, 054018 (2009).
- [3] A. Atre *et al.*, J. High Energy Phys. **1108**, 080 (2011).
- [4] S. Chakdar *et al.* Phys. Rev. D **88**, 095005 (2013).
- [5] H. Fritzsch and D. Holtmannspötter, Phys. Lett. B **457**, 186 (1999).
- [6] G. Aad *et al.* [ATLAS Collaboration], Phys. Rev. Lett. **109**, 032001 (2012).
- [7] S. Chatrchyan *et al.* [CMS Collaboration], Phys.Lett. B718, 307 (2012).
- [8] G. Aad *et al.* [ATLAS Collaboration], arXiv:1409.5500 [hep-ex].
- [9] G. Aad *et al.* [ATLAS Collaboration], Phys. Lett. B **718**, 1284 (2013).
- [10] S. Chatrchyan *et al.* [CMS Collaboration], Phys.Lett. B **716**, 103 (2012).
- [11] G. Aad *et al.* [ATLAS Collaboration], Phys. Lett. B **712**, 22 (2012).
- [12] G. Aad *et al.* [ATLAS Collaboration], JHEP **1211**, 094 (2012).
- [13] S. Chatrchyan *et al.* [CMS Collaboration], Phys.Lett. B **729**, 149 (2014).
- [14] S. Chatrchyan *et al.* [CMS Collaboration], Phys.Rev.Lett. **107**, 271802 (2011).
- [15] G. Aad *et al.* [ATLAS Collaboration], Phys.Lett.B **728** 562 (2014).
- [16] G. Aad *et al.* [ATLAS Collaboration], Phys. Lett. B **721**, 171 (2013).
- [17] R. Ciftci, Phys. Rev. D **78**, 075018 (2008).
- [18] I. T. Cakir, H. Duran Yildiz, O. Cakir and G. Unel, Phys. Rev. D **80**, 095009 (2009).
- [19] E. Arik, O. Cakir and S. Sultansoy, Phys. Rev. D **67**, 035002 (2003).
- [20] M. Sahin, S. Sultansoy, S. Turkoz, Phys. Rev. D **82**, 051503 (2010).
- [21] M. Bobrowski *et al.* Phys. Rev. D **79**, 113006 (2009).
- [22] G. Eilam, B. Melic, J. Trampetic, Phys. Rev. D **80**, 116003 (2009).
- [23] O. Cobanoglu, E. Ozcan, S. Sultansoy, G. Unel, Comp. Phys. Comm. **182**, 1732, (2011).
- [24] A. Belyaev, N. Christensen, A. Pukhov, Comp. Phys. Comm. **184**, 1729 (2013).
- [25] J. Pumplin *et al.* JHEP **0207**, 012 (2002).